Unraveling Mechanistic Differences in Optical and Electrical Sensors: Time-Resolved Operando UV-Vis Spectroscopy of p-Type Perovskite Gas Sensors

*Maximilian Pfeiffer, Christian Hess**

TU Darmstadt, Eduard Zintl Institute of Inorganic and Physical Chemistry, Peter-Grünberg-Str.8, 64287 Darmstadt, Germany

AUTHOR INFORMATION

Corresponding Author

*e-mail: christian.hess@tu-darmstadt.de

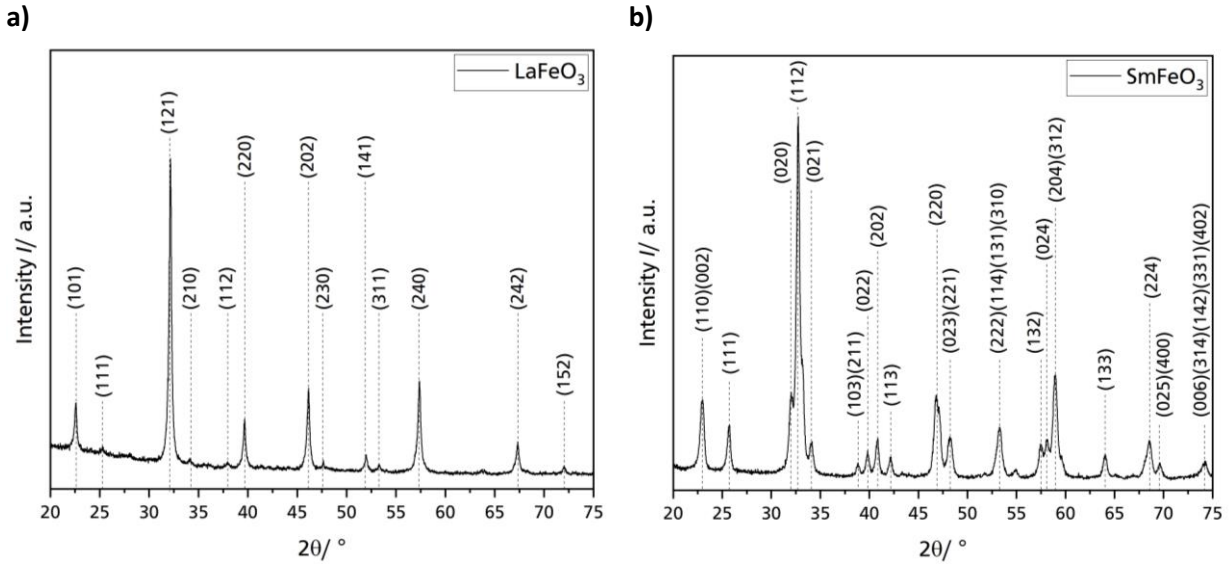

Figure S1. X-ray powder diffractograms of a) $LaFeO_3$ and b) $SmFeO_3$ samples using Cu K_α-radiation (1.5406 Å, 40 kV, 40 mA); indexing of reflexes according to references [1] and [2].

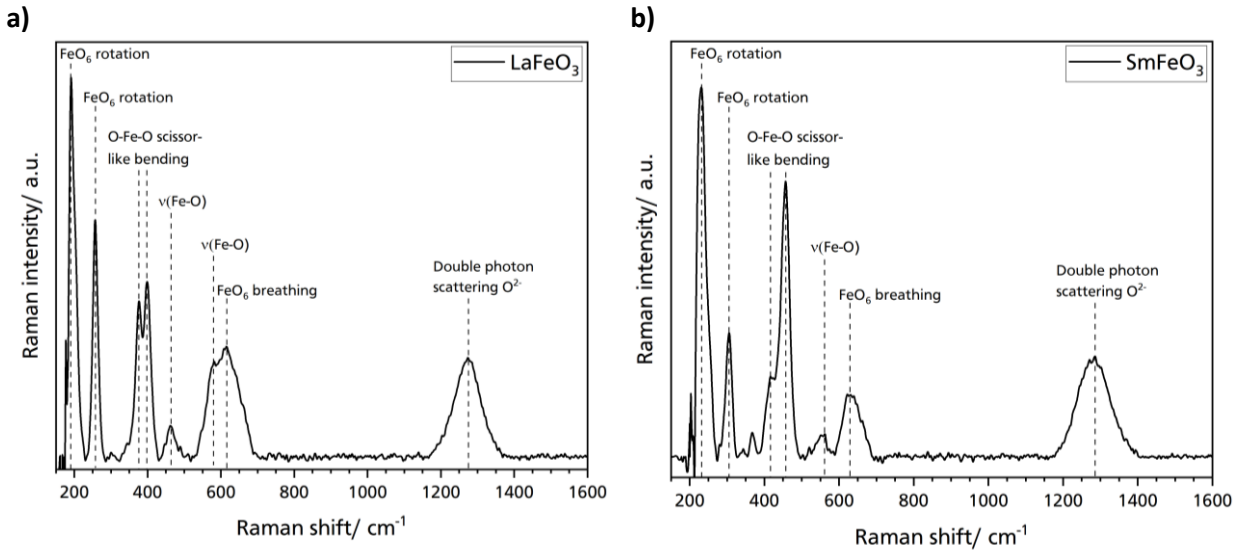

Figure S2. *Ex situ* Raman spectra of a) $LaFeO_3$ and b) $SmFeO_3$ at room temperature (λ_{ext} = 632.8 nm, P = 5 mW, 80 s, 1 Acc.); band assignment according to reference [3].

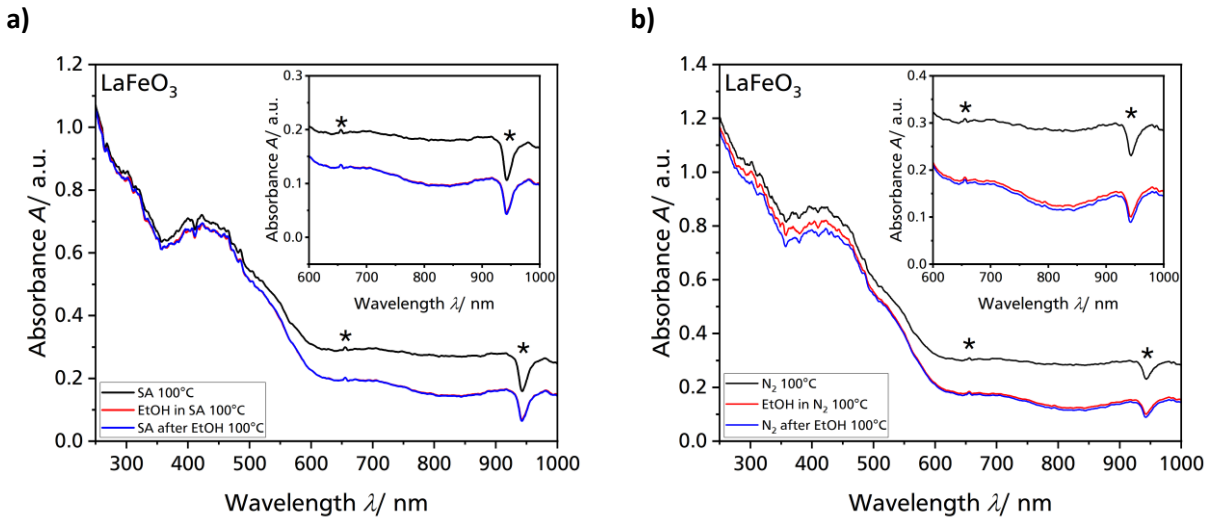

Figure S3. *Operando* UV-Vis spectra of $LaFeO_3$ sensor layer during ethanol sensing at 100 °C using a) synthetic air (80 vol % N_2 + 20 vol % O_2) and b) nitrogen as a carrier gas (total flow rate: 100 ml·min^{-1}). After baking out at 400 °C, the sensor was cooled down to 100 °C (black spectrum). Afterward, 250 ppm of ethanol was added for 40 min (red spectrum), followed by exposure to the respective carrier gas (blue spectrum). An enlarged view of the region 600-1000 nm is found in the upper right corner of a) and b) for better visualization of the changes in free charge carrier absorption due to changes in the gas atmosphere. The asterisks (∗) mark artifacts of the spectrometer. SA: synthetic air; EtOH: ethanol.

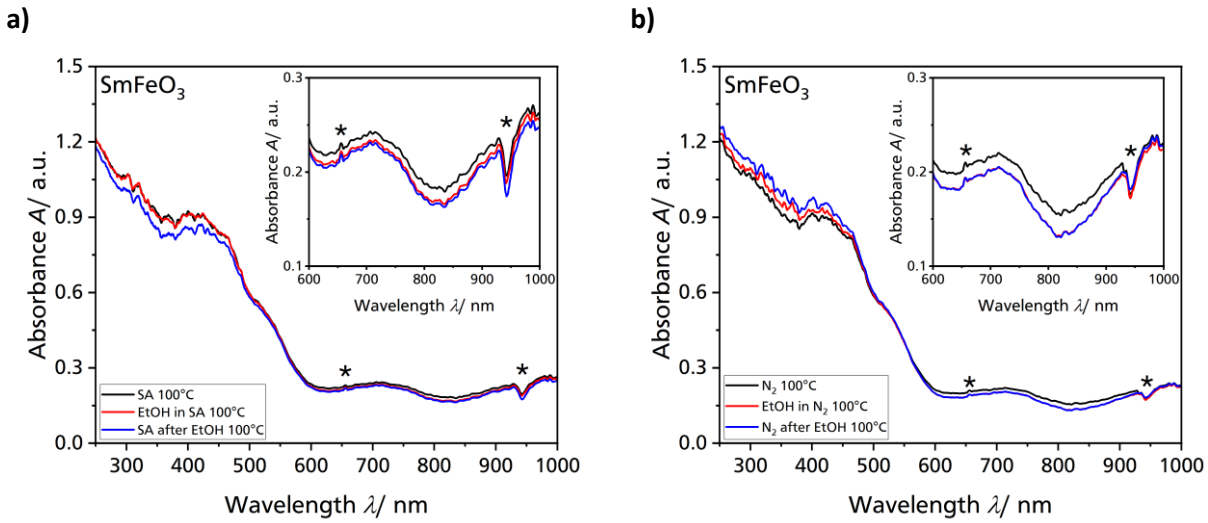

Figure S4. *Operando* UV-Vis spectra of $SmFeO_3$ sensor layer during ethanol sensing at 100 °C using a) synthetic air (80 vol % N_2 + 20 vol % O_2) and b) nitrogen as a carrier gas (total flow rate: 100 ml·min^{-1}). After baking out at 400 °C, the sensor was cooled down to 100 °C (black spectrum). Afterward, 250 ppm of ethanol was added for 40 min (red spectrum), followed by exposure to the respective carrier gas (blue spectrum). An enlarged view of the region 600-1000 nm is found in the upper right corner of a) and b) for better visualization of the changes in free charge carrier absorption to due changes in the gas atmosphere. The asterisks (∗) mark artifacts of the spectrometer. SA: synthetic air; EtOH: ethanol.

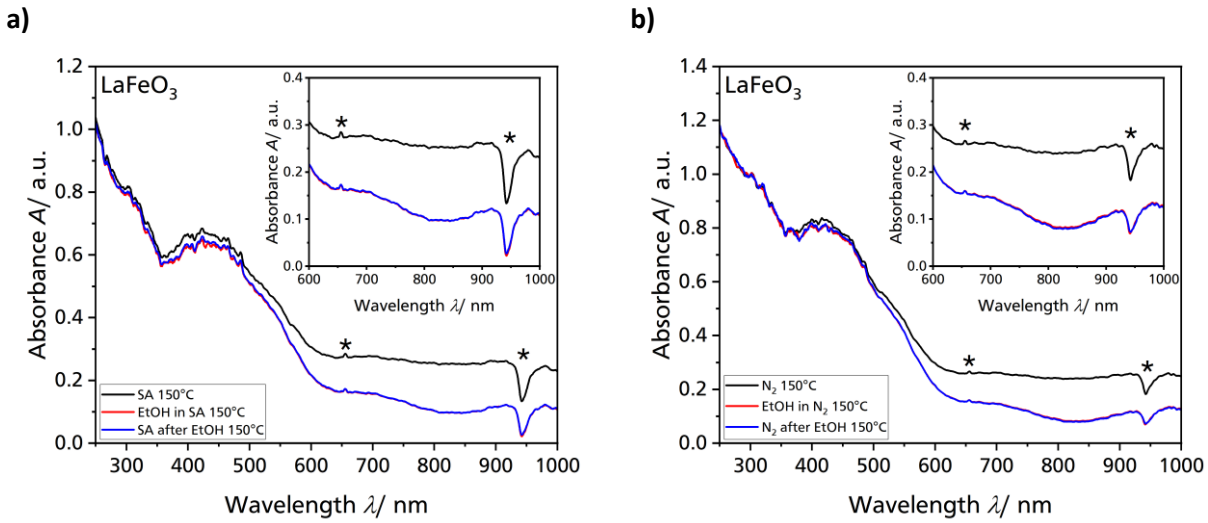

Figure S5. *Operando* UV-Vis spectra of $LaFeO_3$ sensor layer during ethanol sensing at 150 °C using a) synthetic air (80 vol % N_2 + 20 vol % O_2) and b) nitrogen as a carrier gas (total flow rate: 100 ml·min^{-1}). After baking out at 400 °C, the sensor was cooled down to 100 °C (black spectrum). Afterward, 250 ppm of ethanol was added for 40 min (red spectrum), followed by exposure to the respective carrier gas (blue spectrum). An enlarged view of the region 600-1000 nm is found in the upper right corner of a) and b) for better visualization of the changes in free charge carrier absorption due to changes in the gas atmosphere. The asterisks (∗) mark artifacts of the spectrometer. SA: synthetic air; EtOH: ethanol.

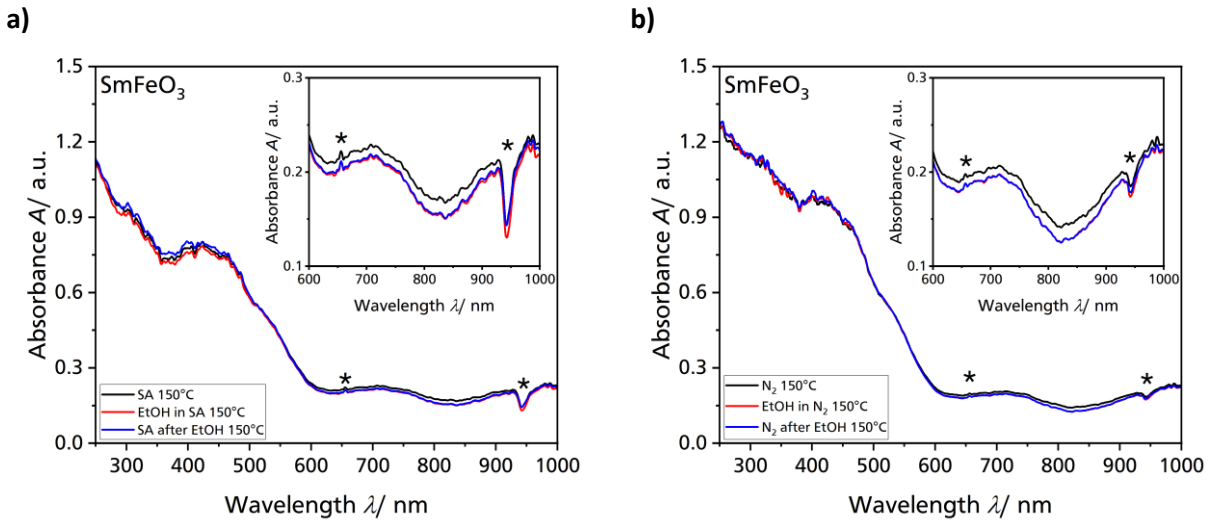

Figure S6. *Operando* UV-Vis spectra of $SmFeO_3$ sensor layer during ethanol sensing at 150 °C using a) synthetic air (80 vol % N_2 + 20 vol % O_2) and b) nitrogen as a carrier gas (total flow rate: 100 ml·min^{-1}). After baking out at 400 °C, the sensor was cooled down to 100 °C (black spectrum). Afterward, 250 ppm of ethanol was added for 40 min (red spectrum), followed by exposure to the respective carrier gas (blue spectrum). An enlarged view of the region 600-1000 nm is found in the upper right corner of a) and b) for better visualization of the changes in free charge carrier absorption due to changes in the gas atmosphere. The asterisks (∗) mark artifacts of the spectrometer. SA: synthetic air; EtOH: ethanol.

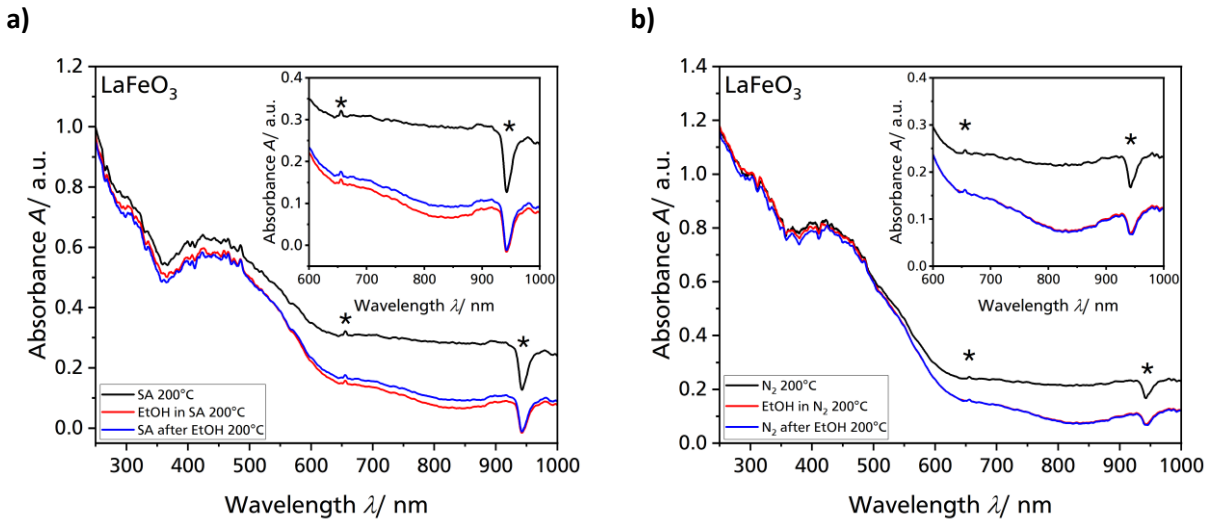

Figure S7. *Operando* UV-Vis spectra of $LaFeO_3$ sensor layer during ethanol sensing at 200 °C using a) synthetic air (80 vol % N_2 + 20 vol % O_2) and b) nitrogen as a carrier gas (total flow rate: 100 ml·min^{-1}). After baking out at 400 °C, the sensor was cooled down to 100 °C (black spectrum). Afterward, 250 ppm of ethanol was added for 40 min (red spectrum), followed by exposure to the respective carrier gas (blue spectrum). An enlarged view of the region 600-1000 nm is found in the upper right corner of a) and b) for better visualization of the changes in free charge carrier absorption due to changes in the gas atmosphere. The asterisks (∗) mark artifacts of the spectrometer. SA: synthetic air; EtOH: ethanol.

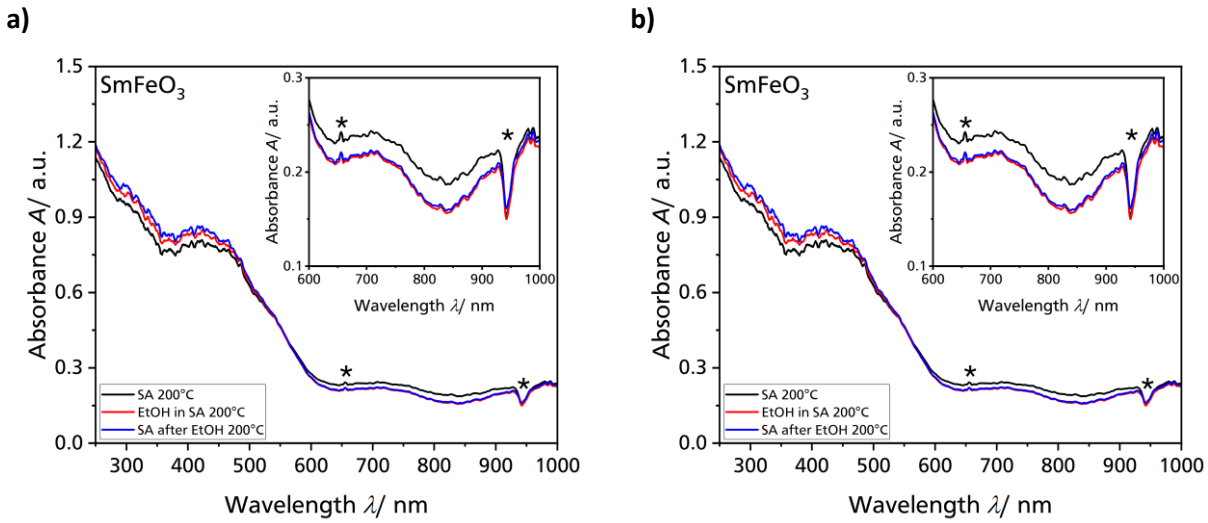

Figure S8. *Operando* UV-Vis spectra of $SmFeO_3$ sensor layer during ethanol sensing at 200 °C using a) synthetic air (80 vol % N_2 + 20 vol % O_2) and b) nitrogen as a carrier gas (total flow rate: 100 ml·min^{-1}). After baking out at 400 °C, the sensor was cooled down to 100 °C (black spectrum). Afterward, 250 ppm of ethanol was added for 40 min (red spectrum), followed by exposure to the respective carrier gas (blue spectrum). An enlarged view of the region 600-1000 nm is found in the upper right corner of a) and b) for better visualization of the changes in free charge carrier absorption due to changes in the gas atmosphere. The asterisks (∗) mark artifacts of the spectrometer. SA: synthetic air; EtOH: ethanol.

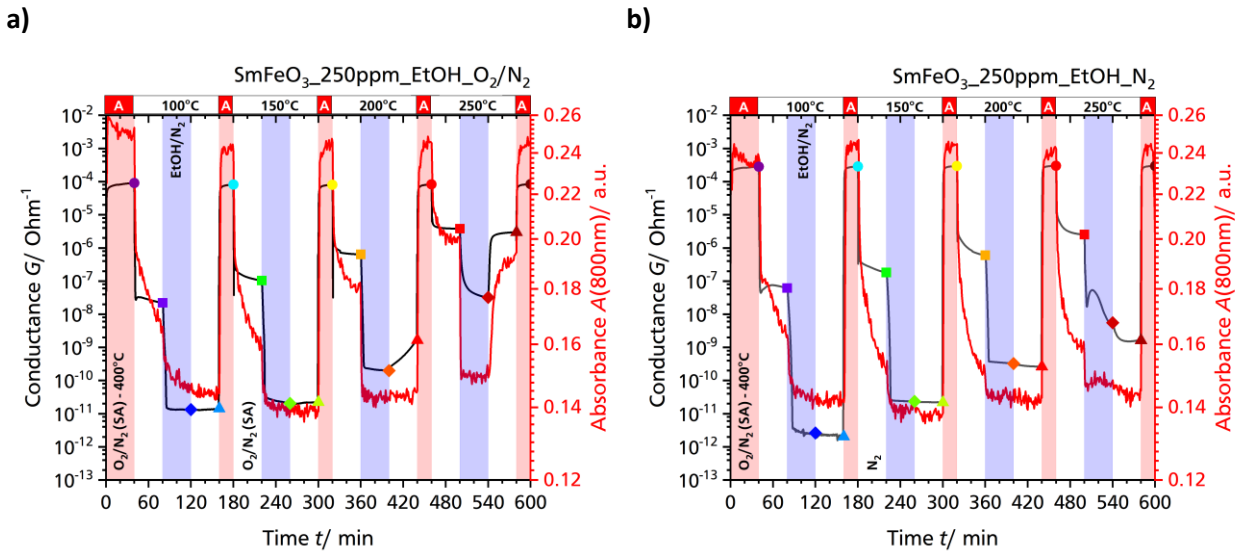

Figure S9. Conductance *G* and absorbance *A* (at 800 nm) of the $SmFeO_3$ sensor during O_2/N_2, N_2 and ethanol exposure using a) synthetic air and b) nitrogen as the carrier gas (total flow rate: 100 mL·min^{-1}). Red areas: heating at 400 °C in synthetic air; white areas: sensor at operating temperature in the respective carrier gas; blue areas: exposure to 250 ppm ethanol in the respective carrier gas; The colored symbols mark the final conductivity values for each phase and serve as an orientation for Fig. S11; SA: synthetic air, EtOH: ethanol.

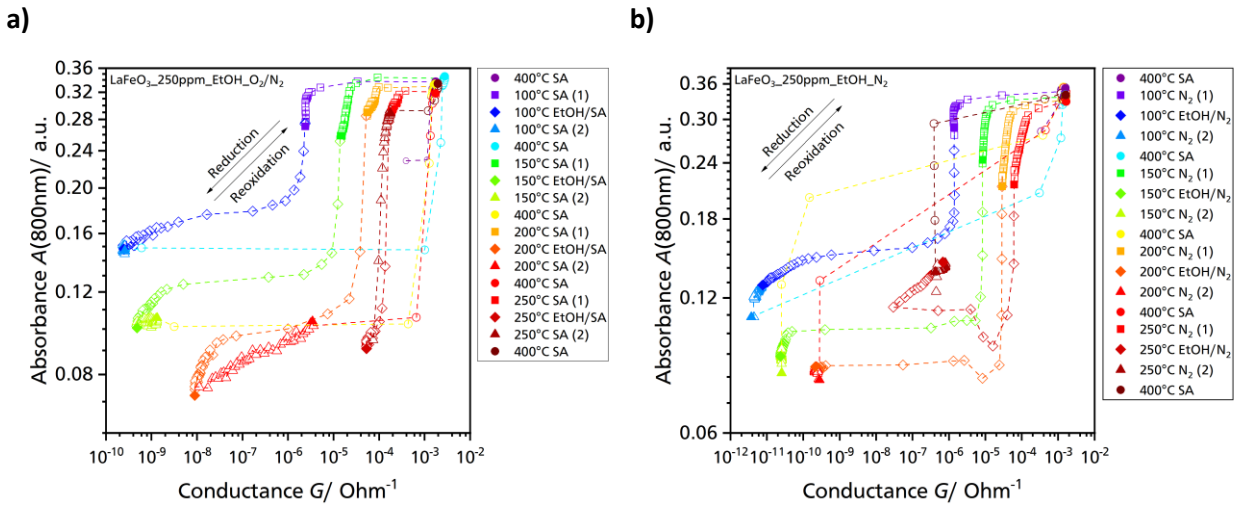

Figure S10. Double logarithmic plot of the absorbance A at 800 nm as a function of the conductance G for the $LaFeO_3$ sensor using a) synthetic air (SA) and b) N_2 as the carrier gas (total flow rate: 100 mL·min^{-1}) during (i) heating out in synthetic air at 400 °C (circles), (ii) cooling down to operation temperature (squares), (iii) exposure to 250 ppm ethanol (EtOH) (diamonds) and (iv) reoxidation after ethanol exposure (triangles); The median value for a time interval of 1 min was plotted for the conductance in each case. The last data point of each phase is marked by a filled-in symbol; the different temperatures are indicated by the different colors of the symbols.

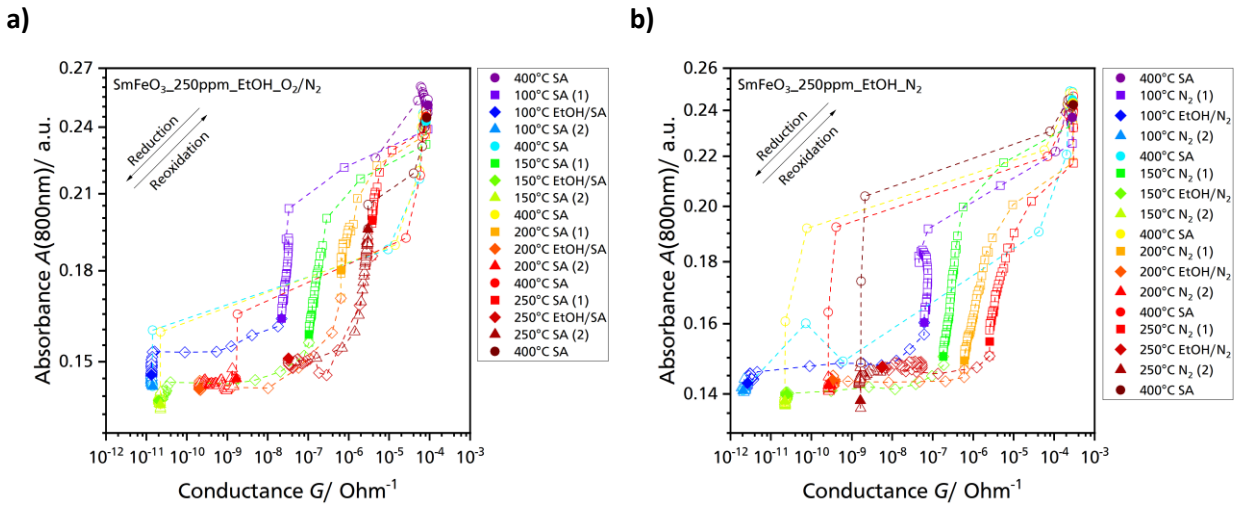

Figure S11. Double logarithmic plot of the Absorbance *A* at 800 nm as a function of the Conductance *G* for the $SmFeO_3$ sensor using a) synthetic air (SA) and b) N_2 as a carrier gas (total flow rate: 100 $mL \cdot min^{-1}$) during (i) heating out in synthetic air at 400 °C (circle), (ii) cooling down to operation temperature (square), (iii) exposure to 250 ppm ethanol (EtOH) (diamond) and (iv) reoxidation after ethanol exposure (triangle); The median value for a time interval of 1 min were plotted for the conductance in each case. The last data point of each phase is marked by a filled-in symbol, the different temperatures are indicated by the different colors of the symbols.

REFERENCES

(1) Jain, P.; Srivastava, S.; Baroliya, I.; Gupta, N. Structure and particle size analysis of $LaFeO_3$ nanoparticles. *AIP Conf. Proc.* **2016**, *1728*, 20659–20662.

(2) Gaiardo, A.; Zonta, G.; Gherardi, S.; Malagù, C.; Fabbri, B.; Valt, M.; Vanzetti, L.; Landini, N.; Casotti, D.; Cruciani, G.*; et al.* Nanostructured $SmFeO_3$ Gas Sensors: Investigation of the Gas Sensing Performance Reproducibility for Colorectal Cancer Screening. *Sensors* **2020**, *20*, 5910–5923.

(3) Weber, M. C.; Guennou, M.; Zhao, H. J.; Íñiguez, J.; Vilarinho, R.; Almeida, A.; Moreira, J. A.; Kreisel, J. Raman spectroscopy of rare-earth orthoferrites $RFeO_3$ (R =La, Sm, Eu, Gd, Tb, Dy). *Phys. Rev. B* **2016**, *94*, 214103-214110.